ROS is also problematic. According to our data, thiourea mildly inhibits cell growth (Fig. 1B), indicating that this compound may have nonspecific effects, such as slowing down cell metabolism, which would lead to increased tolerance to killing. Indeed, we observed protective effect of thiourea from antibiotic killing even under anaerobic conditions (fig. S5). Reports of mutants in the TCA cycle being more resistant to killing could similarly result from these cells having a slower metabolism. Finally, the use of HPF as a detector of ROS is only valid if this dye is a specific detector. However, we find that antibiotics cause a shift in HPF fluorescence under anaerobic conditions (fig. S6). Dying cells apparently produce some products to which HPF responds.

Taken together, our results show that killing by antibiotics is unrelated to ROS production. This finding will refocus efforts on unanswered questions on the mechanism of killing by antibiotics. For example, we do not know how β-lactams induce autolysis, nor how exactly mistranslation caused by aminoglycosides leads to cell death. Better understanding of cell death will guide the development of advanced cures to treat recalcitrant infectious diseases (*23*).

References and Notes

1. I. Keren, D. Shah, A. Spoering, N. Kaldalu, K. Lewis, *J. Bacteriol.* **186**, 8172 (2004).
2. K. Lewis, *Annu. Rev. Microbiol.* **64**, 357 (2010).
3. D. C. Hooper, *Clin. Infect. Dis.* **32** (suppl. 1), S9 (2001).
4. B. D. Davis, L. L. Chen, P. C. Tai, *Proc. Natl. Acad. Sci. U.S.A.* **83**, 6164 (1986).
5. M. A. Kohanski, D. J. Dwyer, J. Wierzbowski, G. Cottarel, J. J. Collins, *Cell* **135**, 679 (2008).
6. K. W. Bayles, *Nat. Rev. Microbiol.* **5**, 721 (2007).
7. T. Uehara, T. Dinh, T. G. Bernhardt, *J. Bacteriol.* **191**, 5094 (2009).
8. M. A. Kohanski, D. J. Dwyer, B. Hayete, C. A. Lawrence, J. J. Collins, *Cell* **130**, 797 (2007).
9. D. J. Dwyer, M. A. Kohanski, J. J. Collins, *Curr. Opin. Microbiol.* **12**, 482 (2009).
10. J. J. Foti, B. Devadoss, J. A. Winkler, J. J. Collins, G. C. Walker, *Science* **336**, 315 (2012).
11. S. S. Grant, B. B. Kaufmann, N. S. Chand, N. Haseley, D. T. Hung, *Proc. Natl. Acad. Sci. U.S.A.* **109**, 12147 (2012).
12. D. Nguyen *et al.*, *Science* **334**, 982 (2011).
13. T. R. Sampson *et al.*, *Antimicrob. Agents Chemother.* **56**, 5642 (2012).
14. Y. Liu *et al.*, *Antimicrob. Agents Chemother.* **56**, 6048 (2012).
15. X. Wang, X. Zhao, *Antimicrob. Agents Chemother.* **53**, 1395 (2009).
16. B. Poolman, *FEMS Microbiol. Rev.* **12**, 125 (1993).
17. J. Hoskins *et al.*, *J. Bacteriol.* **183**, 5709 (2001).
18. R. C. Rowen, D. J. Michel, J. C. Thompson, *Pharmacotherapy* **7**, 92 (1987).
19. G. Unden, J. Bongaerts, *Biochim. Biophys. Acta* **1320**, 217 (1997).
20. P. D. Damper, W. Epstein, *Antimicrob. Agents Chemother.* **20**, 803 (1981).
21. J. M. Andrews, *J. Antimicrob. Chemother.* **48** (suppl. 1), 5 (2001).
22. C. Wiuff *et al.*, *Antimicrob. Agents Chemother.* **49**, 1483 (2005).
23. K. Lewis, *Nature* **485**, 439 (2012).

Acknowledgments: The authors thank V. Isabella for helpful discussion of the manuscript. This work was supported by NIH grant T-R01AI085585-01 and by Army Research Office grants W9911NF-09-1-0265 and 55631-LS-RIP.

Supplementary Materials

www.sciencemag.org/cgi/content/full/339/6124/1213/DC1
Materials and Methods
Figs. S1 to S6
Reference (*24*)

13 November 2012; accepted 24 January 2013
10.1126/science.1232688

Evidence for a Common Mechanism of SIRT1 Regulation by Allosteric Activators

Basil P. Hubbard,[1] Ana P. Gomes,[1,2] Han Dai,[3] Jun Li,[1] April W. Case,[3] Thomas Considine,[3] Thomas V. Riera,[3] Jessica E. Lee,[4] Sook Yen E,[4] Dudley W. Lamming,[1]* Bradley L. Pentelute,[5] Eli R. Schuman,[3] Linda A. Stevens,[6] Alvin J. Y. Ling,[1] Sean M. Armour,[1] Shaday Michan,[1]† Huizhen Zhao,[7] Yong Jiang,[7] Sharon M. Sweitzer,[7] Charles A. Blum,[3] Jeremy S. Disch,[3] Pui Yee Ng,[3] Konrad T. Howitz,[8]‡ Anabela P. Rolo,[2,9] Yoshitomo Hamuro,[4] Joel Moss,[6] Robert B. Perni,[3] James L. Ellis,[3] George P. Vlasuk,[3] David A. Sinclair[1,10]§

A molecule that treats multiple age-related diseases would have a major impact on global health and economics. The SIRT1 deacetylase has drawn attention in this regard as a target for drug design. Yet controversy exists around the mechanism of sirtuin-activating compounds (STACs). We found that specific hydrophobic motifs found in SIRT1 substrates such as PGC-1α and FOXO3a facilitate SIRT1 activation by STACs. A single amino acid in SIRT1, Glu^{230}, located in a structured N-terminal domain, was critical for activation by all previously reported STAC scaffolds and a new class of chemically distinct activators. In primary cells reconstituted with activation-defective SIRT1, the metabolic effects of STACs were blocked. Thus, SIRT1 can be directly activated through an allosteric mechanism common to chemically diverse STACs.

The nicotinamide adenine dinucleotide (NAD^+)–dependent deacetylase SIRT1 is implicated in the prevention of many age-related diseases such as cancer, Alzheimer's disease, and type 2 diabetes (*1*). At the cellular level, SIRT1 controls DNA repair and apoptosis, circadian clocks, inflammatory pathways, insulin secretion, and mitochondrial biogenesis (*2*, *3*).

Naturally occurring STACs such as resveratrol (*4*) and chemically unrelated synthetic STACs activate SIRT1 in vitro by lowering its peptide Michaelis constant (K_M) and produce pharmacological changes consistent with SIRT1 activation (*4*–*7*). However, the legitimacy of STACs as direct SIRT1 activators has been widely debated. In previous studies, STACs increased SIRT1 activity toward fluorophore-tagged substrates but not toward corresponding nontagged peptides (*8*–*11*). One explanation was that STACs were binding to the fluorophore-linked substrate, which would not occur in vivo (*10*). Alternatively, the fluorescent groups might mimic a property of natural substrates. Given that the fluorophores used in previous studies are bulky and hydrophobic (*4*, *5*), we tested whether these moieties might substitute for hydrophobic amino acids in endogenous substrates.

We used a SIRT1 activity assay whereby the reaction product nicotinamide was converted to 1-alkylthio–substituted isoindoles via the nicotinamidase PNC1 (*12*) and ortho-phthalaldehyde (OPT) (*13*) (fig. S1, A to E). A second assay measured the SIRT1 product *O*-acetyl adenosine diphosphate ribose (OAcADPR) by mass spectrometry (*14*) (fig. S2, A to E).

A series of STACs, including STAC-1 (SRT1460) (*5*) and STAC-2 [compound 22 in (*15*)] (fig. S3), activated SIRT1 with an aminomethylcoumarin (AMC)–tagged peptide serving as a substrate via a peptide K_M-lowering mechanism, similar to the action of resveratrol (fig. S4, A to C, and tables S1 and S2) (*4*). The AMC moiety mediated activation only when it was directly adjacent to the acetylated Lys^9 of histone 3 (H3K9) at the +1 position (*16*); this finding demonstrates that the fluorophore has a positional requirement (Fig. 1A and fig. S5A). The fluorophore moieties at

[1]Department of Genetics, Harvard Medical School, Boston, MA 02115, USA. [2]Center for Neurosciences and Cell Biology, Department of Life Sciences, University of Coimbra, Coimbra 3004-517, Portugal. [3]Sirtris, a GSK Company, Cambridge, MA 02139, USA. [4]ExSAR Corporation, Monmouth Junction, NJ 08852, USA. [5]Department of Chemistry, Massachusetts Institute of Technology, Cambridge, MA 02139, USA. [6]NIH Cardiovascular and Pulmonary Branch/National Heart, Lung and Blood Institute, Bethesda, MD 20892, USA. [7]GlaxoSmithKline, Collegeville, PA 19426, USA. [8]BIOMOL Research Laboratories Inc., Plymouth Meeting, PA 19462, USA. [9]Department of Biology, University of Aveiro, Aveiro 3810-193, Portugal. [10]Department of Pharmacology, University of New South Wales, Sydney, NSW 2052, Australia.

*Present address: Whitehead Institute for Biomedical Research, Cambridge, MA 02142, USA.
†Present address: Instituto Nacional de Geriatría, Institutos Nacionales de Salud, México D.F. 04510, México.
‡Present address: Reaction Biology Corporation, Malvern, PA 19355, USA.
§To whom correspondence should be addressed. E-mail: david_sinclair@hms.harvard.edu

positions +1 (*4*) or +6 (*5*) were dispensable if replaced with naturally occurring hydrophobic amino acids (*15*) (Fig. 1B and fig. S5B).

We then tested whether native peptide sequences might also support activation (*17*–*24*). Sequences from two SIRT1 substrates supported STAC-mediated activation: mouse peroxisome proliferator–activated receptor γ coactivator 1α Lys^{778} (PGC-1α–K778) (*22*) and human forkhead box O3a protein Lys^{290} (FOXO3a-K290) (*19*) (Fig. 1C). STAC-mediated activation was dose-dependent (Fig. 1D), and relative activation was similar between the SIRT1 assays (fig. S5C).

Isothermal titration calorimetry (ITC) did not detect binding between saturating amounts of PGC-1α peptide (2 mM) and STAC-1 (100 μM) or STAC-2 (50 μM), arguing against activation driven solely by substrate enhancement (fig. S6, A and B) (*15*). Kinetic analysis of SIRT1 activation by STAC-2 with the FOXO3a-K290 substrate revealed that rate enhancement was mediated primarily through a lowering of peptide K_M (fig. S6C). Thus, the mechanism of activation appeared to be independent of the substrate used.

The PGC-1α–K778 peptide contains aromatic, hydrophobic amino acids at the +1 and +6 positions (relative to the acetylated lysine), as does the FOXO3a-K290 peptide at position +1. Alanine substitution of either the Tyr at the +1 position or the Phe at the +6 position of the PGC-1α peptide reduced activation, and substitution of both abolished activation completely (Fig. 2A). Similarly, for FOXO3a, substitution of the Trp at the +1 position blocked activation (Fig. 2B), but substitution of several N-terminal residues did not (Fig. 2, A and B). A global search of nuclear acetylated proteins, conforming to the sequences X_6-K(Ac)-{Y,W,F}-X_5, X_6-K(Ac)-X_5-{Y,W,F} (*16*), and the union of the two sets, identified more than 400 sequences (fig. S7A). We tested five of these native sequences and found that three of them supported activation: metallothionein-like 5 (MTL5), peptidylprolyl isomerase A (PPIA), and eukaryotic translation initiation factor 2α (eIF2α) (*25*) (fig. S7B).

An alternative peptide sequence from FOXO3a (encompassing Lys^{242}) was sequentially altered to resemble the FOXO3a-K290 sequence. Substitution of the Ser at +1 with Trp did not impart the ability to activate (fig. S7C) unless in combination with a Pro substitution at the +2 position (fig. S7C). Thus, a hydrophobic residue at the +1 position is necessary but not sufficient for activation.

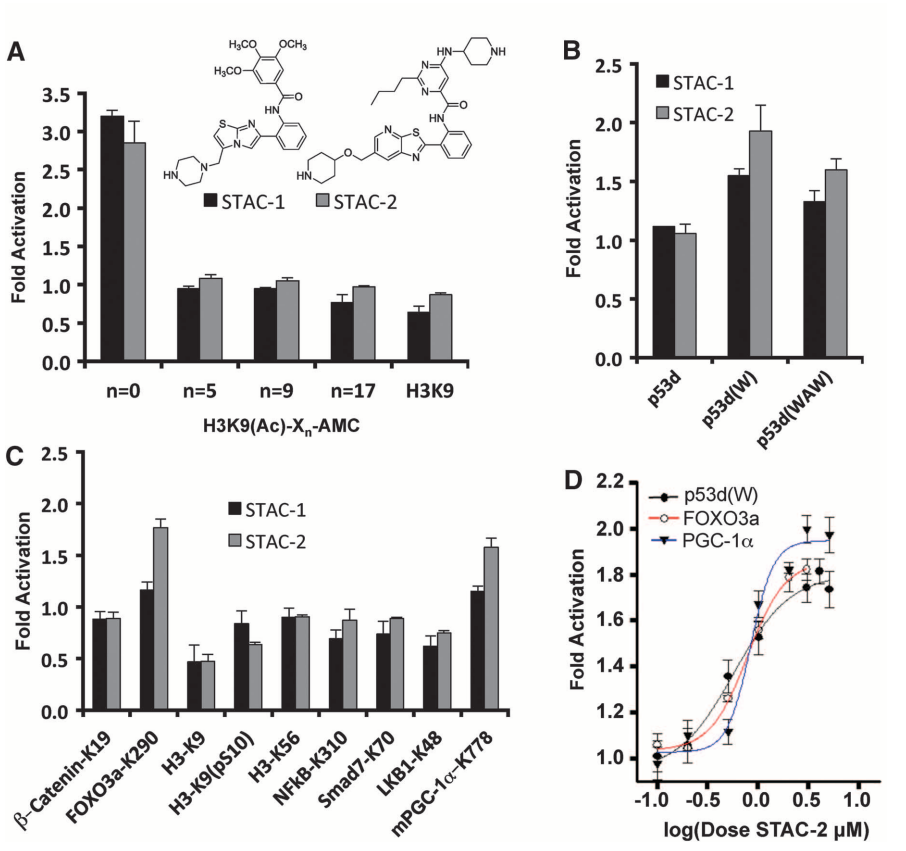

Fig. 1. SIRT1 activation by STACs on native peptide sequences. (**A**) SIRT1 activation by 50 μM STAC-1 or 5 μM STAC-2 with peptides bearing an AMC moiety at the indicated positions, where X_n represents the number of amino acids between the acetylated lysine and the AMC. (**B**) SIRT1 activation by STACs on hydrophobic patch peptides. Complete amino acid sequences of peptides bearing tryptophan (W) or tryptophan and alanine substitutions (WAW) are provided in the supplementary materials. (**C**) SIRT1 activation on native peptide sequences of known targets (detailed in the supplementary materials). (**D**) Dose-response curves for STAC-2 as measured by PNC1-OPT assay; data are means ± SEM (n = 3).

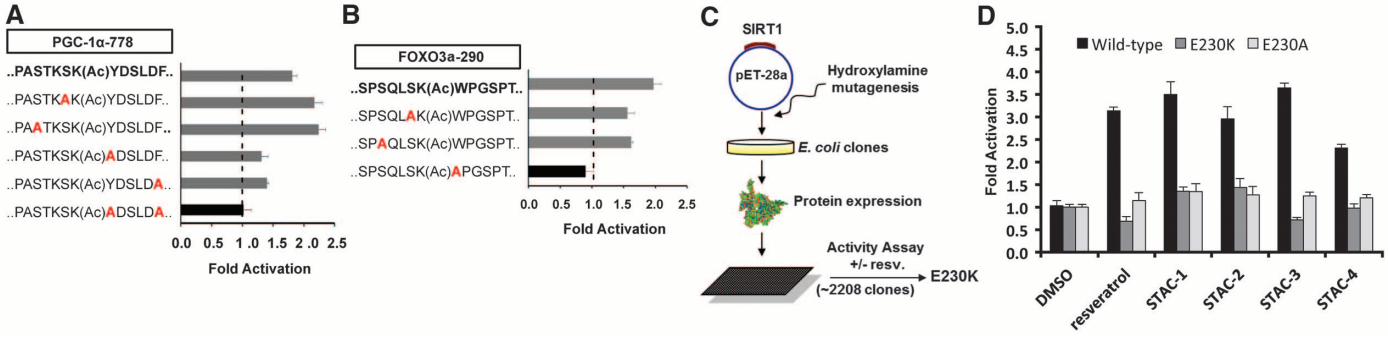

Fig. 2. Substrate sequence requirements and regions on SIRT1 necessary for activation. (**A** and **B**) SIRT1 activation by STAC-2 on peptides derived from PGC-1α–K778 (A) and FOXO3a-K290 (B) as measured by PNC1-OPT assay; data are means ± SEM (n = 3). (**C**) Biochemical screen for activation-compromised mutants. A bacterial expression plasmid (pET28a) carrying the SIRT1 gene was mutagenized and used to generate recombinant SIRT1 proteins that were screened for activity in the presence or absence of resveratrol using an AMC-based assay. (**D**) Activation of wild-type SIRT1, E230K, and E230A mutants by 40 μM resveratrol, 50 μM STAC-1, 5 μM STAC-2, 5 μM STAC-3, and 10 μM STAC-4 as measured by an AMC assay; data are means ± SD (n = 3). Dimethyl sulfoxide (DMSO) was used as a control.

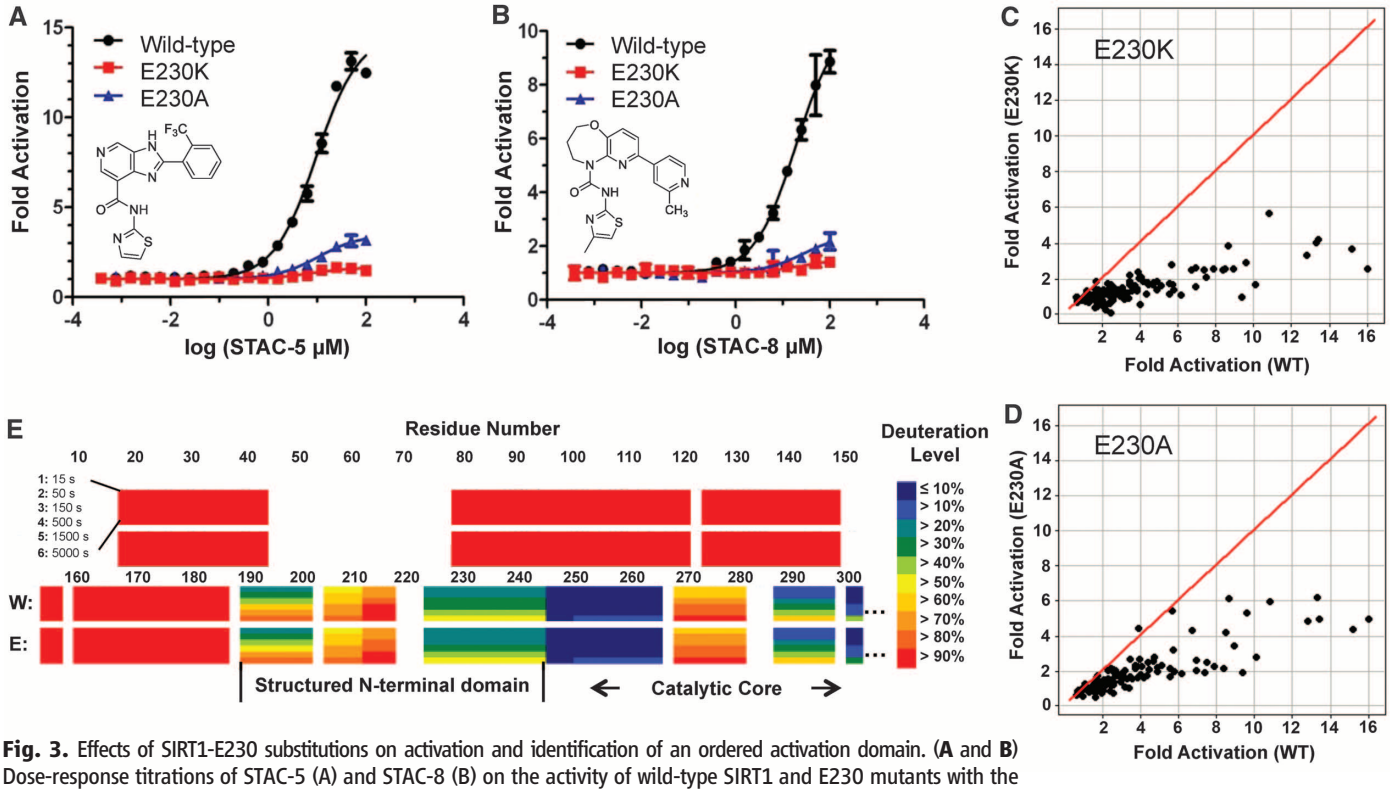

Fig. 3. Effects of SIRT1-E230 substitutions on activation and identification of an ordered activation domain. (**A** and **B**) Dose-response titrations of STAC-5 (A) and STAC-8 (B) on the activity of wild-type SIRT1 and E230 mutants with the Trp 5-mer peptide serving as the substrate, as measured by mass spectrometry–based OAcADPR assay. The sequence of the Trp 5-mer peptide is included in the supplementary materials. data are means ± SD (n = 3). (**C** and **D**) Relative activation by a chemically diverse, 117-compound set (25 μM) using the Trp 5-mer substrate for wild-type versus E230K (C) or wild-type versus E230A (D), as measured by OAcADPR assay (n = 2). The red line represents $y = x$ correlation. (**E**) HDXMS heat map of deuteration levels of wild-type (W) and SIRT1-E230K (E) N termini at six different time points (15 to 5000 s).

These data were consistent with an allosteric mechanism of SIRT1 activation (*4*, *15*). To elucidate the determinants of activation in SIRT1, we screened for SIRT1 mutant proteins lacking activation (Fig. 2C). The ability of SIRT1 to be activated by resveratrol was attenuated in one mutant that substituted a lysine for a glutamate at position 230 (E230K), whether an AMC-tagged substrate (Fig. 2D) or a natural amino acid substrate was used (fig. S8A). Substitution of Glu^{230} with Lys or Ala attenuated SIRT1 activation by 117 chemically diverse STACs, independent of the substrate used (Fig. 2D, Fig. 3, A to D, fig. S8, B and C, and tables S3 and S4).

Glu^{230} is immediately N-terminal to the catalytic core of SIRT1 and is conserved from flies to humans (fig. S8D). The E230K substitution did not impair the basal catalytic activity of SIRT1, nor did it significantly alter the maximum velocity of reaction (V_{max}), the Michaelis constant for NAD^+ ($K_{M\ NAD^+}$), or the K_M for several peptides (fig. S9, A to E) or the median inhibitory concentration (IC_{50}) values for several SIRT1 inhibitors (fig. S10, A to E and table S5). Secondary structural elements, thermal denaturation profiles (fig. S11, A to C and table S6), melting temperatures (fig. S12, A and B), and intracellular localization patterns (fig. S13A) of wild-type and SIRT1-E230K were also similar.

To examine the entire structure of SIRT1, we used hydrogen-deuterium exchange mass spectrometry (HDXMS). No changes in protein dynamics were detected between wild-type and SIRT1-E230K. The catalytic core domain showed slow exchange, consistent with a well-defined structure (fig. S14, A and B). The N and C termini showed fast exchange (fig. S14A), except for a small C-terminal region around residue 650 recently implicated in the regulation of SIRT1 activity (*26*, *27*) and a small rigid N-terminal region, residues 190 to 244, encompassing Glu^{230} (Fig. 3E and fig. S14A).

The variable median effective concentration (EC_{50})/dissociation constant (K_d) ratios indicate that the majority of synthetic STACs do not interact strongly with SIRT1 and likely bind to a steady-state form such as the enzyme-substrate complex (*15*). SIRT1 truncations of the first 183 residues did not disrupt STAC binding, but truncations to residues 195 and 225 did, coincident with a loss of activation (table S7), whereas the E230K substitution had variable effects on STAC binding (fig. S15). Together, these data indicate that SIRT1 has a structured N-terminal domain that is required for STAC binding that encompasses Glu^{230}, an amino acid critical for activation across a broad class of STACs.

Resveratrol and synthetic STACs increase mitochondrial function in a SIRT1-dependent manner (*28*–*30*). However, it is unclear whether this is a direct or indirect effect of STACs on SIRT1. We therefore reconstituted primary SIRT1 knockout (KO) myoblasts (*30*) with wild-type mouse SIRT1 or mouse SIRT1-E222K (the murine equivalent of human SIRT1-E230K) (Fig. 4A and fig. S16A). STACs increased mitochondrial mass and adenosine triphosphate (ATP) content in wild-type but not SIRT1 KO myoblasts (Fig. 4, B and C, and fig. S16B). In myoblasts carrying SIRT1-E222K, the effects of STACs on mitochondrial mass and ATP levels were also blocked (Fig. 4, B and C, and fig. S16B). In SIRT1 KO mouse embryonic fibroblasts (MEFs) reconstituted with SIRT1-E222K (fig. S17A), the ability of STACs to increase mitochondrial mass, ATP, and mitochondrial DNA copy number was also blocked (fig. S17, B to D, and fig. S18A). At these concentrations, there was no evidence for SIRT1-independent adenosine monophosphate (AMP)–activated protein kinase phosphorylation (fig. S19A) (*30*) or inhibition of phosphodiesterase isoforms (table S8). These findings argue against these pathways directly mediating the effects of STACs.

The data presented here favor a mechanism of direct "assisted allosteric activation" mediated by an N-terminal activation domain in SIRT1 (fig. S20, A and B) that is responsible for at least some of the physiological effects of STACs. Thus, allosteric activation of SIRT1 by STACs remains a viable therapeutic intervention strategy for many diseases associated with aging.

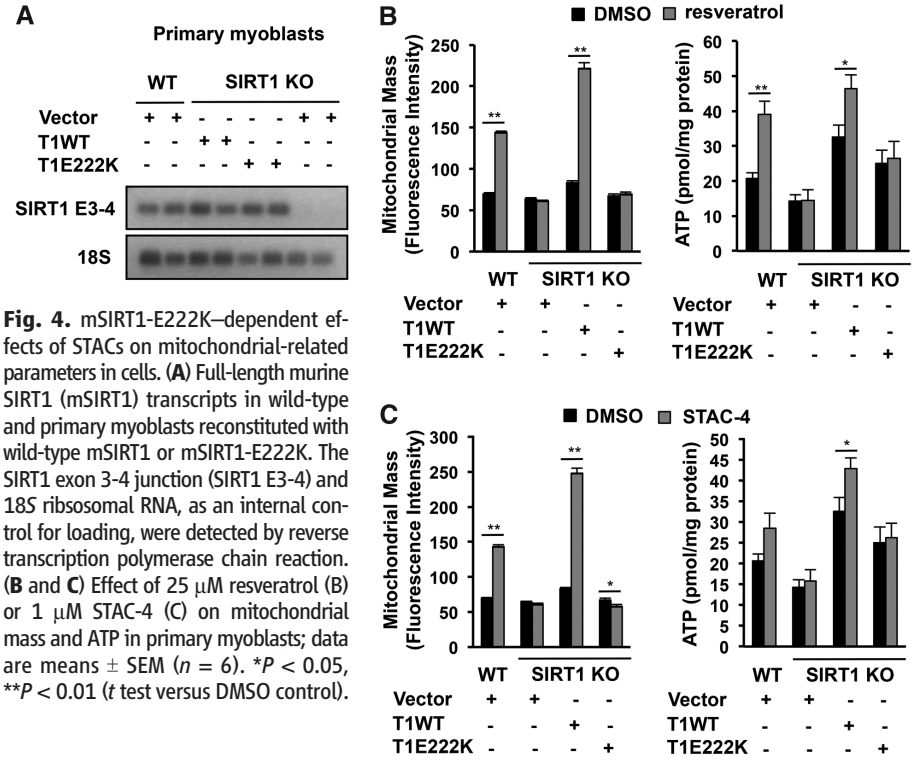

Fig. 4. mSIRT1-E222K–dependent effects of STACs on mitochondrial-related parameters in cells. (**A**) Full-length murine SIRT1 (mSIRT1) transcripts in wild-type and primary myoblasts reconstituted with wild-type mSIRT1 or mSIRT1-E222K. The SIRT1 exon 3-4 junction (SIRT1 E3-4) and 18*S* ribsosomal RNA, as an internal control for loading, were detected by reverse transcription polymerase chain reaction. (**B** and **C**) Effect of 25 μM resveratrol (B) or 1 μM STAC-4 (C) on mitochondrial mass and ATP in primary myoblasts; data are means ± SEM ($n = 6$). *$P < 0.05$, **$P < 0.01$ (t test versus DMSO control).

References and Notes

1. C. Sebastian, K. F. Satterstrom, M. C. Haigis, R. Mostoslavsky, *J. Biol. Chem.* **287**, 42444 (2012).
2. M. C. Haigis, D. A. Sinclair, *Annu. Rev. Pathol.* **5**, 253 (2010).
3. A. Chalkiadaki, L. Guarente, *Nat. Rev. Endocrinol.* **8**, 287 (2012).
4. K. T. Howitz *et al.*, *Nature* **425**, 191 (2003).
5. J. C. Milne *et al.*, *Nature* **450**, 712 (2007).
6. J. A. Baur *et al.*, *Nature* **444**, 337 (2006).
7. R. K. Minor *et al.*, *Sci. Rep.* **1**, 70 (2011).
8. M. Kaeberlein *et al.*, *J. Biol. Chem.* **280**, 17038 (2005).
9. M. T. Borra, B. C. Smith, J. M. Denu, *J. Biol. Chem.* **280**, 17187 (2005).
10. M. Pacholec *et al.*, *J. Biol. Chem.* **285**, 8340 (2010).
11. D. Beher *et al.*, *Chem. Biol. Drug Des.* **74**, 619 (2009).
12. M. Ghislain, E. Talla, J. M. François, *Yeast* **19**, 215 (2002).
13. K. Sugawara, F. Oyama, *J. Biochem.* **89**, 771 (1981).
14. A. A. Sauve, C. Wolberger, V. L. Schramm, J. D. Boeke, *Annu. Rev. Biochem.* **75**, 435 (2006).
15. H. Dai *et al.*, *J. Biol. Chem.* **285**, 32695 (2010).
16. Single-letter abbreviations for amino acid residues: A, Ala; C, Cys; D, Asp; E, Glu; F, Phe; G, Gly; H, His; I, Ile; K, Lys; L, Leu; M, Met; N, Asn; P, Pro; Q, Gln; R, Arg; S, Ser; T, Thr; V, Val; W, Trp; Y, Tyr; X, any amino acid.
17. A. Vaquero *et al.*, *Mol. Cell* **16**, 93 (2004).
18. R. Firestein *et al.*, *PLoS ONE* **3**, e2020 (2008).
19. A. Brunet *et al.*, *Science* **303**, 2011 (2004).
20. S. Kume *et al.*, *J. Biol. Chem.* **282**, 151 (2007).
21. F. Lan, J. M. Cacicedo, N. Ruderman, Y. Ido, *J. Biol. Chem.* **283**, 27628 (2008).
22. J. T. Rodgers *et al.*, *Nature* **434**, 113 (2005).
23. F. Yeung *et al.*, *EMBO J.* **23**, 2369 (2004).
24. C. Das, M. S. Lucia, K. C. Hansen, J. K. Tyler, *Nature* **459**, 113 (2009).
25. H. S. Ghosh, B. Reizis, P. D. Robbins, *Sci. Rep.* **1**, 150 (2011).
26. H. Kang *et al.*, *Mol. Cell* **44**, 203 (2011).
27. M. Pan, H. Yuan, M. Brent, E. C. Ding, R. Marmorstein, *J. Biol. Chem.* **287**, 2468 (2012).
28. Z. Gerhart-Hines *et al.*, *EMBO J.* **26**, 1913 (2007).
29. M. Bernier *et al.*, *J. Biol. Chem.* **286**, 19270 (2011).
30. N. L. Price *et al.*, *Cell Metab.* **15**, 675 (2012).

Acknowledgments: Supported by the Glenn Foundation for Medical Research, the Ellison Medical Foundation, the Juvenile Diabetes Research Foundation, the United Mitochondrial Disease Foundation, NIH and NIAID grants, an NSERC fellowship (B.P.H.), the Portuguese Science and Technology Foundation (A.P.G.), the Intramural Research Program, and NIH/NHLBI (L.A.S. and J.M.). D.A.S. is a consultant and inventor on patents licensed to Sirtris, a GSK company. H.D., A.W.C., T.C., T.V.R., E.R.S., H.Z., Y.J., S.M.S., C.A.B., J.S.D., P.Y.N., R.B.P., J.L.E., and G.P.V. are employees of Sirtris, a GSK company. Dedicated to the memories of Jana Perni and Harmon Rasnow. A patent application on the PNC1-OPT sirtuin assay has been filed by Harvard Medical School with D.A.S. and B.P.H. as inventors. Patent applications related to sirtuin activators have been filed by Sirtris and Biomol. Natural Sirt1 activators will be provided upon request. Synthetic STACs are provided under a material transfer agreement from Sirtris.

Supplementary Materials

www.sciencemag.org/cgi/content/full/339/6124/1216/DC1
Materials and Methods
Figs. S1 to S20
Tables S1 to S8
Reference (*31*)

4 October 2012; accepted 18 January 2013
10.1126/science.1231097

Aire-Dependent Thymic Development of Tumor-Associated Regulatory T Cells

Sven Malchow,[1] Daniel S. Leventhal,[1] Saki Nishi,[1] Benjamin I. Fischer,[1] Lynn Shen,[1] Gladell P. Paner,[1] Ayelet S. Amit,[1] Chulho Kang,[2] Jenna E. Geddes,[3]* James P. Allison,[3]† Nicholas D. Socci,[4] Peter A. Savage[1]‡

Despite considerable interest in the modulation of tumor-associated Foxp3$^+$ regulatory T cells (T_{regs}) for therapeutic benefit, little is known about the developmental origins of these cells and the nature of the antigens that they recognize. We identified an endogenous population of antigen-specific T_{regs} (termed MJ23 T_{regs}) found recurrently enriched in the tumors of mice with oncogene-driven prostate cancer. MJ23 T_{regs} were not reactive to a tumor-specific antigen but instead recognized a prostate-associated antigen that was present in tumor-free mice. MJ23 T_{regs} underwent autoimmune regulator (Aire)–dependent thymic development in both male and female mice. Thus, Aire-mediated expression of peripheral tissue antigens drives the thymic development of a subset of organ-specific T_{regs}, which are likely coopted by tumors developing within the associated organ.

Regulatory T (T_{reg}) cells are critical for the prevention of autoimmunity, the maintenance of immune homeostasis, and the suppression of antitumor immune responses (*1*, *2*). For many human cancers, the density of T_{regs} within tumor lesions is predictive of poor clinical outcome (*3*), suggesting that T_{regs} play a functional role in cancer progression. In this study, we set out to establish a tractable animal model in which a single specificity of naturally occurring tumor-associated T_{regs} could be studied in the context of a genetically driven mouse model of autochthonous cancer. In order to identify an endogenous tumor-associated T_{reg} response, we analyzed the immune response in TRAMP mice, which develop prostatic adenocarcinoma because of the transgenic expression of the model oncogene SV40 T antigen in the prostate (*4*, *5*). Unlike the prostates of tumor-free mice, which contain very few

[1]Department of Pathology, University of Chicago, Chicago, IL 60637, USA. [2]Cancer Research Laboratory, University of California, Berkeley, CA 94720, USA. [3]Department of Immunology, Howard Hughes Medical Institute, Memorial Sloan-Kettering Cancer Center, New York, NY 10021, USA. [4]Bioinformatics Core, Memorial Sloan-Kettering Cancer Center, New York, NY 10021, USA.

*Present address: Department of Immunology, Harvard Medical School, Boston, MA 02115, USA.
†Present address: Department of Immunology, The University of Texas MD Anderson Cancer Center, Houston, TX 77030, USA.
‡To whom correspondence should be addressed. E-mail: psavage@bsd.uchicago.edu